Clumped hydrogen anomalies at cryogenic temperatures

Frederik Felius

Supervisor: M.E. Popa

June 2019

Abstract

Molecular hydrogen is considered an indirect greenhouse gas. In normal isotopic analysis, only the the more abundant molecule of HD is considered, and the clumped isotopologue D_2 is neglected, due to the low mixing ratio. Clumped isotopes are important when considering geological processes, or processes at or near thermodynamic equilibrium. In this work I determine the clumping anomaly of molecular hydrogen in the cryogenic region, with gases near atmospheric abundance ratios.
Experiments were conducted between the -196°C and 350°C range, with a focus between -196° and -78°C. Clumping anomaly for this focus range is between +1000 to +385 ‰, and experiments had a typical precision in range of $2-5$ ‰. The low temperature experiments in this range underestimated the clumping anomaly compared to theoretical predictions, whereas the mid to high temperature of this range agrees with predictions. The clumping anomalies have been determined to be independent of the bulk isotopic composition of the gas, and independent of previous clumping state of the gas. It is only a property of the equilibrium temperature of the gas. A change of temperature may partially explain the deviation from theoretical prediction, but is not consistent over the experiment set. Conducted experiments have been verified by creating gases with known clumping anomaly. These experiments agreed with the predictions.

Contents

1 Introduction

In the study of greenhouse gases, it is also important to consider the indirect greenhouse gases. Molecular hydrogen (H_2) is considered an indirect greenhouse gas due to its reaction with the OH-radical, and subsequently increasing the lifetime of other greenhouse gases, such as carbon-monoxide (CO).

As hydrogen is present in many different processes, such as (bio)chemical, geological or pyrogenic processes. A way of examining these processes is to investigate the isotopic composition of an atmospheric air sample. Hydrogen has three isotopes: Protium (^1H), deuterium (^2H or D), and the unstable tritium (^3H or T). I neglect the unstable tritium in this work, as this work is interested in stable isotopes.

The relative abundances of deuterium and hydrogen atoms are 0.015% and 99.985% respectively. These atoms form into the following molecules: H_2, HD and D_2, note that HD has two possible configurations. When detecting this molecule, it is not known if either the HD or DH configuration is measured.

Chemical processes discriminate between the different isotopologues of a molecule, as kinetic processes are mass dependent. This fractionation is unique to every process, and measuring the relative abundance of the isotopes can be used to fingerprint the processes of a sample. On the other hand, the distribution of the isotopes over the isotopologues yields information of the underlying processes. In true stochastic equilibrium it would be 99.7% for H_2, 0.3% for HD (two possible configurations), and 2.25×10^{-4} % for D_2.

The distribution of the isotopologues can be determined through the partition function. This is an energy and temperature dependent function, and governs the equilibrium of the hydrogen isotopologues through the Boltzmann factor:

$$Q(E_i, T) \propto e^{\frac{-E_i}{k_B T}} \tag{1}$$

with E_i denoting the energy of the specific system state, k_B the Boltzmann constant, and T the absolute temperature. from the evaluation of the partition function, the thermodynamic properties of a system can be derived.

The difference in zero point energy of the isotopologues cause the difference between equilibrated molecular hydrogen, and stochastic equilibrium. As differences in energy levels are magnified with decreasing temperature, the largest anomalies are found in the low temperature region.

This becomes clear when the Boltzmann factor is written out as:

$$Q(E_i, T) \propto e^{\frac{-1}{k_B T} E_i} \tag{2}$$

Where the only difference between isotopologues is found in E_i. With decreasing temperature, the derivative of the Boltzmann factor increases. Making it interesting to investigate the molecular clumping at low temperatures.

1.1 Goal

In this work, I develop an experimental scale for the clumping anomaly in hydrogen gas, using the MAT253+ Ultra present at the Institute for Marine and Atmospheric science Utrecht (IMAU).The Ultra is an high resolution mass spectrometer, able to differentiate molecules with the same nominal mass.
The experimental results are compared with theoretical prediction of clumping anomaly, as derived from statistical physics. The conducted experiments will be verified by creating a gas with known clumping anomaly, and determine the clumping anomaly of this gas.

2 Method

2.1 Definitions

For the reporting of isotopic composition of molecules, the following definitions will be used:

$$\delta D = (\frac{R_{sample}}{R_{reference}} - 1) \times 1000 \tag{3}$$

$$= (\frac{(\frac{D}{H})_{sample}}{(\frac{D}{H})_{reference}} - 1) \times 1000 \ [‰] \tag{4}$$

And for the clumped isotope:

$$\delta DD = (\frac{(\frac{DD}{HH})_{sample}}{(\frac{DD}{HH})_{reference}} - 1) \times 1000[‰] \tag{5}$$

Where the reference is either the working gas used, or Vienna Mean Standard Ocean Water (VSMOW), the international standard with an abundance ratio of $D/H = 155.76 \pm 0.1$ ppm. It is easily done to calibrate a working gas for δD, but no calibrated gases against VSMOW exist for δDD, this makes it impossible to convert to international standard during this research. Instead it will be converted to an absolute scale.

The anomaly is defined as the deviation from the stochastic ratio of clumped deuterium. That is, the measured ratio of D_2 is compared to the expected statistical ratio of D_2. As per standard in isotope analysis, this metric is converted into permil by the relation:

$$\Delta DD = (\frac{(DD/HH)_m}{(DD/HH)_e} - 1) \times 1000 \ \ [‰] \tag{6}$$

Where subscript m denotes measured, and e denotes expected. Assuming that the expectation is in stochastic equilibrium, it follows that this relation can be rewritten as:

$$\begin{aligned}(DD/HH)_e &= (\frac{D \times D}{H \times H})_e \\ &= (\frac{D}{H}_e) \times (\frac{D}{H})_e = (\frac{D}{H})_e^2 \end{aligned} \tag{7}$$

To relate the absolute ratio of these isotopes to a measurable quantity, it can be converted as:

$$(\frac{D}{H})_e \approx 0.5 \times (\frac{HD}{HH})_m \tag{8}$$

This is approximately true, but not exact. As due to the anomaly, part of the HD content is consumed by the DD content. But this is of very small effect, as there is a difference of 10^4 between the intensities of the isotopologues, due to the small abundance ratio of deuterium. With experimental uncertainties being (much) larger than this inequality, it is safely neglected in the analysis during this study.
The anomaly is subsequently reduced to:

$$\Delta DD \approx (4 \times \frac{(DD/HH)_m}{(\frac{D}{H})_m^2} - 1) \times 1000 \text{ [‰]} \tag{9}$$

Each of the detectors used in this study has an amplifier and a sensitivity. This makes it impossible to directly use the intensity of the isotopologues to compute the clumping anomaly. To remove this issue, two operations are performed.
The first one being that the ratios of molecules are replaced by the standard delta-values of the measured gas. This introduces a division of the ratios of the sample and working gas, thus cancelling out the sensitivity of the detectors. The relation becomes:

$$\begin{aligned}\delta DD &= \frac{(\frac{\alpha \times DD}{\beta \times HH})_{sample}}{(\frac{\alpha \times DD}{\beta \times HH})_{ref}} \\ &= \frac{\alpha \times \beta \times DD_s \times HH_r}{\alpha \times \beta \times DD_r \times HH_s} r \qquad (10) \\ &= \frac{DD_s \times HH_r}{DD_r \times HH_s} \qquad (11)\end{aligned}$$

Where α and β are arbitrary, but stationary, sensitivities of the detectors. In the calculation of δ-values of a gas, these divide out.
As the δ values of a gas is relative to the reference gas used, this has to be converted to an absolute scale. This can be done if the reference gas is calibrated. If the reference gas is calibrated, the measured clumping anomaly can be con-

verted to an absolute anomaly by the relation:

$$\Delta DD_m = (\frac{(\frac{\delta DD}{1000} + 1)}{(\frac{\delta D}{1000} + 1)^2} - 1) \times 1000 \text{ [‰]} \tag{12}$$

$$\Delta DD_{abs} = \Delta DD_m + \Delta DD_{ref} + \frac{\Delta DD_m \times \Delta DD_{ref}}{1000} \tag{13}$$

So the gas is first measured against the reference gas, and has a relative ΔDD_m value against the reference gas. It is subsequently converted to an absolute scale by using relation 13. The reference gas is calibrated using a temperature with known clumping anomaly, and this is subsequently assigned to that gas.

2.2 Instrumental details

During this work we made use of the MAT253+ Ultra present at IMAU, henceforth abbreviated to Ultra. The Ultra is a high resolution mass spectrometer, able to differentiate molecules sharing the same nominal mass, but of different composition. Examples of such molecules are $^{13}CH_4$ and $^{12}CDH_3$. Though these share the same nominal mass (17), due to the different combination of isotopes there is a slight mass difference between these isotopologues.

The Ultra is outfitted with an interchangeable slit, to control the resolution of the ion beam. The slit width affects the signal intensity of the beam passing through (narrower leads to less intensity), but increases the resolution of the beam (better focused ion beam). During this work, the medium resolution slit ($16\mu m$) has been used, as different isotopologues were clearly distinguishable, and for maximizing signal intensity.

The molecules have to be distinguished from the adduct peaks formed in the source of the Ultra. In figure 1 a scan of these masses are shown, with the relevant molecules indicated. At the start of an experiment, the magnetic field is set by determining the mass of the center cup (non-moveable). As the required magnetic field can change over time, a peak center procedure is employed.
The peak center procedure determines the center of the H_2 peak, and is applied to all other masses. That is, if mass 2 drifts by $10^{-3}\mu$, all other center masses are updated with the same drift.
For small drifts this is reasonable and the measurement will still be on the plateaus as seen in figure 1. However, the masses do not drift uniformly, and there is a difference in the magnitude of the shift. It is possible that during the experiment, adduct peaks will be measured instead of the isotopologue. These measurements are subsequently removed from the results, and are no longer considered.

The Ultra is outfitted with 9 (8 movable and 1 stationary) Faraday cups and 4 (3 movable and 1 stationary) ion counters. These are able to measure

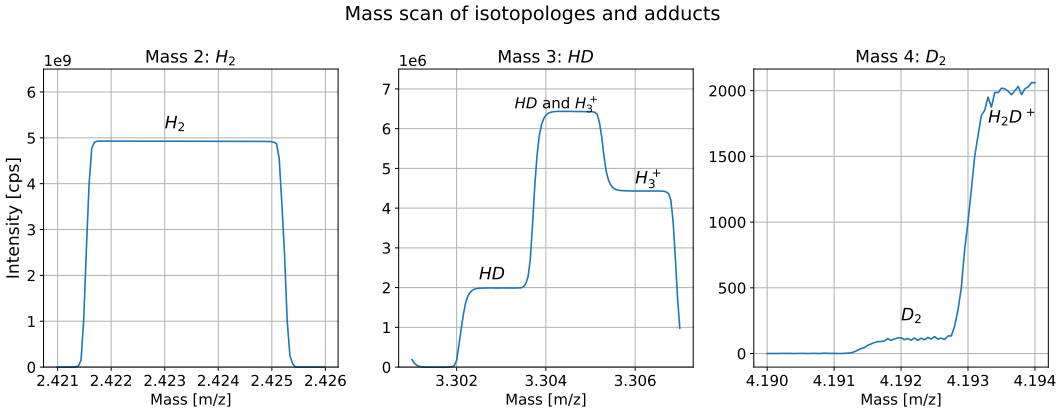

Figure 1: Mass scan of the isotopologues. On the x-axis the mass over charge ratio, y-axis the measured intensity. Measurement plateaus are indicated in the figures, with the adducts next to them. The intensity difference makes it obvious when measuring on the adduct.

simultaneously.
However, due to the large relative mass difference between the hydrogen isotopologues (50 and 100%), these cannot be measured simultaneously in the same magnetic field. To solve this, the isotopologues are measured sequentially, but with fixed positions of the measuring cups. The magnetic field is adjusted between measurements of the isotopologues.

2.2.1 Measurement method

The isotopologues are measured in sequence, in the order: H_2, HD, $D_{2,short}$, D_2, H_2, HD. The $D_{2,short}$ was introduced to stabilize the CDD counter used for the D_2 isotopologue. The bellows are measured in sequence, starting and ending with the reference bellow to average results of this bellows to determine the isotopic values of the sample gas.
There are three limiting factors for the experiments:
1) During the switch between isotopologues, Qtegra, the acquisition program for the Ultra, could encounter an error and stop measuring the isotopologues. This yielded shorter experiments with less datapoints at best.
2) The non-uniform drift of peaks could cause measurement to be placed on the adducts. All datapoints measured on the adduct were useless and mostly the whole experiment is discarded.
3) The depletion rate of hydrogen is large, with comparison to other molecular gases. Combined with long integration times for the D_2 isotopologue, this yielded insufficient gas for long measurements. Later datapoints were subject to the nonlinearity of the Ultra, and not useable for further analysis.

During the whole of the research, the quick depletion of the pressure was the limiting factor for measurements of the isotopologues.

2.2.2 Pressure adjust

Over the experiments, two different methods were used to adjust the pressure of the bellows. In the first method, pressure was adjusted on both bellows before measuring the bellows. In this sequence, the sample bellow is measured twice, surrounded by measurements of the reference bellow. In the calculations for the isotopic values, the averages of surrounding reference measurements are used.
Pressure in the bellow will slowly decrease over these five measurements, but this averaging procedure corrects for this. After the measurements, the peak center is determined and pressures are adjusted.
The pressure adjustment of this method is performed on the measured intensity of the H_2 isotopologue, resulting in both bellows to have the same intensity. The tolerance of this method is 1% of the signal.

A second method became available for the May experiment set. This adjusts the pressure of the bellow before the measurement of the bellow, instead of at the start of a sequence of measurements. The pressure is adjusted to a predetermined pressure of the bellow, not intensity measured. Both bellows have a different intensity with bellow pressure due to the crimp present in the system, and have to be set individually at the start of an experiment. The resulting intensities of the signal are within 3% of the desired signal intensity.
This method has two key advantages. First is the measurement speed. This adjustment is performed with 10 seconds, where the previous pressure adjustment took more than a minute. The second advantage is that this removes pressure dependence of the isotopic values. Measurements performed with the previous method showed pressure dependence in the isotopic values, but it is corrected for in subsequent data analysis.
The major drawback of this method is that the bellows deplete of gas quicker. As pressure is kept constant, the flowrate does not decrease.

2.3 Experimental details

During the experiments, two different methods to cool the samples has been employed. In the first experiment set conducted in February, traditional cooling baths have been used. These were:

- Liquid nitrogen: $-195.79°C$
- Dry ice + ethanol: $-78°C$
- Ice + water: $0°C$

These cooling baths retain temperature, regardless of the volume of coolant present.
During the experiment set of May, a cooling device has been used. This was

a hollow copper cylinder, cooled with liquid nitrogen, and kept at temperature with heating wires. This device is described in appendix A.

For heating experiments, a small cylindrical oven has been used, with temperatures between 50 and 850°C able to be maintained.

2.3.1 Used material

Hydrogen was equilibrated in quartz tubes, fused to a glass Young valve. The catalysts (described below) are placed in the bottom of the tube. It is assumed that re-equilibration only occurs at the catalyst, rendering gas above the catalyst inactive. The length of the quartz tubes was approximately 25-30 cm, the quartz-glass fusing a few cm, and the glass connection with young valve approximately 8 cm. The connection to the Ultra was a 1/4" glass tube, connected with an Ultra-torr connector.

2.3.2 Cr_2O_3 catalyst

In previous work [3] Cr_2O_3 powder has been used as catalyst to facilitate reaction 20, and this was used as a starting point for catalysis selection during this work. Fused lumps of Cr_2O_3 were commercially bought from *Alfa Aesar*. One of the key qualifiers for our catalyst was that it had to be a non-powdered substance.

Though reaction rate depends of the available catalytic surface, the direct connection to the Ultra with the reaction tubes posed too large a risk to permanently contaminate the bellows. On contamination of the bellows, the hydrogen gas would undergo re-equilibration inside the bellow and no equilibria could be measured.
A precaution has been taken by placing screens between the tube and the tubing leading to the Ultra.

The Cr_2O_3 lumps were carefully placed inside the quartz tubes, to not contaminate the glass parts, and were subsequently brought under a hydrogen atmosphere. For the catalyst activation, multiple procedures were tried.

The procedure followed by *Gould et al., 1934* [3] was placing the catalyst inside the reaction vessel, and reducing it in a pure H_2 atmosphere at 340°C for 32 hours.

Three tubes had Cr_2O_3 administered, and were subsequently evacuated for 2 hours with the high-vacuum pump, to evacuate the catalyst. Heated to 350°C, and brought under a H_2 atmosphere (IMAU-line gas), and reduced between 20 and 40 hours.

Between different fillings, the tube was evacuated while heated at 350°C, flushed with H_2, and filled at 350°C before bringing it to room temperature.

2.3.3 Platinum on carbon catalyst

The second set of catalysts were supplied by *Peter Ngene* from the chemistry department of Utrecht University. The first of these catalysts were platinum nanoparticles (2%) on carbon, compressed from a fine powder to flat discs, without the use of a binder.
The second of these catalysts were palladium nanoparticles (1%) on carbon, compressed in the same way.

In order to insert the catalyst in the quartz tubes, the discs had to be broken. This caused small fragments, some of which were near powdered. To reduce contamination risk, only larger fragments were retained. During the placing of catalyst of the first experiment set, the shard tended to stick to the walls of the quartz tube.
After exposing the tube to a vacuum pump, catalyst stuck to the quartz tube tended to drop to the bottom of the tube. It is possible that the catalyst caused H_2O to form, making it stick to the walls.

Due to time constraints, and the fracturing of the palladium discs, only the platinum catalyst was used during this work. The catalyst was conditioned by bringing it to 300°C under a hydrogen atmosphere, and flushing the catalyst for approximately 20 minutes. As the tubes only had one opening, flushing was performed by filling the tube with hydrogen, and subsequently evacuating it, repeating this action over the course of 20 minutes.

2.3.4 Equilibrium time

In order to be certain if a sample is at thermodynamic equilibrium, an estimate has to be made of the equilibrium time. It is assumed that the reaction rate increases with increasing temperature, thus the lowest will be found at liquid nitrogen temperature.
To investigate this, a tube was filled to "normal" pressure (1.2 bar absolute), and brought to liquid nitrogen temperature, and sampled after 1 hour, and 3.5 hours (separate fillings). The former of these two experiments measured a clumping anomaly of $\Delta DD = 878‰$, and the latter experiment gave $\Delta DD = 1014‰$, which seems to be at equilibrium.
A first estimate places the equilibration time at 2 hours, so samples measured (at liquid nitrogen temperature) with equal or longer equilibrium times are assumed to be in thermodynamic equilibrium.
Note that the equilibrium time is dependent on the catalytic surface available. The more powdered the Pt on carbon catalyst becomes, the more catalytic surface available per mass unit. During the different experiment sets (February

and May) the catalyst was placed in different tubes, and only larger shards were retained during the May experiments (lowering the catalytic surface available, increasing the equilibrium time).

2.3.5 Gases

Two gases have been used during this research.
The first is a large cylinder, referred to as the IMAU H2 line gas during this work, with nominal isotopic value of $-150‰$ in δD Preliminary measurements by *Popa et al*[8] indicated that the clumping anomaly of this gas is equilibrated near room temperature. An initial value of 240‰ has been assigned for preliminary investigation of the data.

The second gas was a small calibration cylinder, labeled NAT360. Nominal value for $\delta D = +205 \pm 2.16‰$. This was an extremely anomalous gas in its δDD content. Measurements conducted by *E. Popa et al.*[8] placed initial clumping anomaly around 26.000‰

2.3.6 Conducted experiments

Experiments were conducted to determine:

- Cryogenic clumping anomaly
- Heated clumping anomaly
- Independence of ΔDD_{eq} of
  - bulk isotopic composition
  - $\Delta DD_{initial}$
- ΔDD of mixed gases

The cooling and heating experiments were conducted to determine the clumping anomaly of equilibrated hydrogen. Experiments were conducted with two different gases to show that the bulk isotopic composition does not determine the clumping anomaly of the gas.
Most experiments started at room temperature, before bringing it to the equilibrium temperature. To investigate the effect of past clumping anomaly, hysteresis experiments were conducted. These experiments equilibrated samples at temperatures lower than the final temperature, e.g. liquid nitrogen before dry ice + ethanol cooling baths.
All experiments above are performed to determine the equilibrated clumping anomaly. A clumping anomaly can be created by mixing gases. This is independently verify the results obtained in experiments above, as the clumping anomaly can be predicted for these experiments (see section 3.3)

2.4 Error analysis

2.4.1 Counting statistics

The theoretical limit for precision in the measurements is found in the shot noise, which follows the Poisson-distribution. In the measurement of the HD isotopologue, only one integration is made, but in the measurement of the DD isotopologue 5 integrations of 33.55 seconds are made, and averaged. The uncertainties are added as follows:

$$\begin{aligned}\sigma_{N_i} &= (\Sigma_{i=1}^{N}(\sigma_i)^2)^{1/2} \\ &= (\Sigma_{i=1}^{N}(\sqrt{t\times < n_i >}^2)^{1/2} \\ &= (t \times \Sigma_{i=1}^{N} < n_i >)^{1/2} \\ &= (t \times N \times < N_i >)1/2 \\ &= (t_{integration} \times < N_i >)^{1/2}\end{aligned} \tag{14}$$

Where N is the number of intergrations, t the time of one individual integration, $t_{integration}$ the total integration time, n_i the number of counts of an individual integration, N_i the number over all integrations, and <> denotes the averaging procedure, that is:

$$< N_i > = \frac{\Sigma_{i=1}^{N} n_i}{N} \tag{15}$$

The expected uncertainty, expressed in ‰ is given by:

$$\sigma_{SE} = \frac{\sqrt{\Sigma_{i=1}^{N}(\frac{1000}{\sqrt{<N_i>\times t_{integration}}})^2}}{\sqrt{M}} \tag{16}$$

where M denotes the number of measurements performed to obtain this uncertainty. This relation takes explicitly into account the differing number of counts of the gases used. As the different gases had different bulk isotopic composition, the signal intensity between the gases differed. This relation takes the shot noise induced due to the different gases explicitly into account by summing over the individual shot noises.

2.4.2 Propagation of uncertainties

As the clumping anomaly is calculated through the isotopic values of the gases, the expected uncertainty of the clumping anomaly has to be determined through propagation of the expected uncertainties.
Errors are propagated through the relation:

$$\sigma_{\Delta DD} = \sqrt{\Sigma_{i=1}^{N}(\frac{\partial \Delta DD}{\partial x_i} \times \sigma_{x_i})^2} \tag{17}$$

where x_i denotes a variable on which ΔDD depends, and σ_{x_i} its respective uncertainty. Recall that the clumping anomaly is defined as:

$$\Delta DD_{abs} = \Delta DD_{measured} + \Delta DD_{ref} + \frac{\Delta DD_{measured} \times \Delta DD_{ref}}{1000}[‰] \tag{18}$$

$$\Delta DD_{measured} = (\frac{(\frac{\delta DD_{measured}}{1000} + 1)}{(\frac{\delta D_{measured}}{1000} + 1)^2} - 1) \times 1000[‰]$$

During a measurement, the assigned value of the reference gas does not change, so this does not induce an uncertainty in the measurement itself, but does in the eventual result. To evaluate this relation, it can be abbreviated to the form:

$$\begin{aligned} F(\delta D, \delta DD, \Delta DD_{ref}) &= \text{eq.}(18) \\ \frac{\partial F}{\partial \delta D} &= \frac{-2(\frac{\delta DD}{1000} + 1)}{(\frac{\delta D}{1000} + 1)^3} \times (1 + \frac{\Delta DD_{ref}}{1000}) \\ \frac{\partial F}{\partial \delta DD} &= \frac{1}{(\frac{\delta D}{1000} + 1)^2} \times (1 + \frac{\Delta DD_{ref}}{1000}) \\ \frac{\partial F}{\partial \Delta DD_{ref}} &= (1 + \frac{\Delta DD_{measured}}{1000}) \end{aligned}$$

Using these relations, the expected uncertainty in the ΔDD can be computed, and compared to the standard error of the measurements.

2.4.3 Bias correction

During the experiment set of May, the bellows of the Ultra exhibited a bias. In δD this bias can easily be determined, as it was of the order 1‰, with standard error being much smaller.
For δDD this bias not obvious between measurements. Only when averaging over measurements performed during the May experiments, the bias becomes visible. In figure 2 the results of zero-enrichment experiments are shown to track the bias.
A zero-enrichment experiment consists of measuring the same gas in both bellows, against each other. If the bellows exhibit no bias, the enrichment of the measurement should be zero.
Over the measurement set, δD slowly drifted (the bias becomes worse with time), in δDD this drift is not obvious due to the large errors associated with the D_2 measurements.

To correct for a bias in the bellows, the measured sample is calculated as if measured against reference gas in the same bellow. This relation is:

$$\delta(C, B) = \frac{\delta(C, A) - \delta(B, A)}{\delta(B, A) + 1} \tag{19}$$

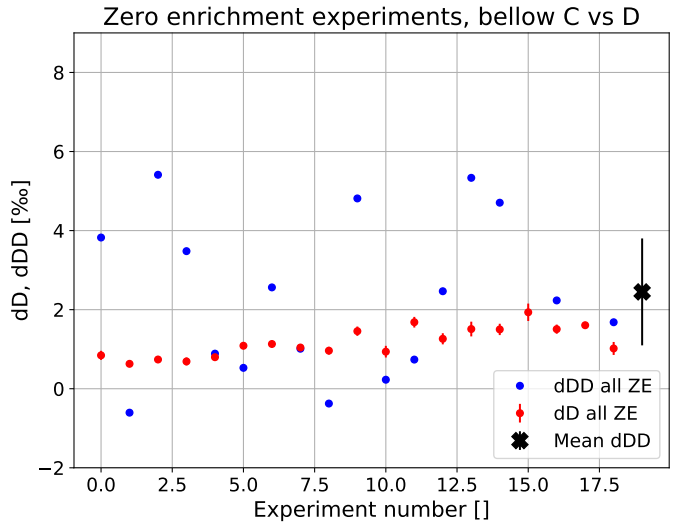

Figure 2: Zero enrichment measurements during the May set. δD is plotted with standard error, δDD is not to keep the figure readable. The mean of δDD is shown with the standard error (and corrected with the Student factor).

For correction in δD the next determination of the bias is applied on the previous experiments. For correction in δDD the average is used to apply on the May dataset.

2.5 Calibration of reference gas

The calibration of the reference gas has been performed in two different methods:

- Direct calibration for the May experiments
- Retroactive calibration for the February experiments

The direct calibration for the May experiments was performed by equilibrating NAT360 with the Pt/C catalyst at ice-water temperature. For this experiment, a clumping anomaly of 256.25‰ has been assigned to the equilibrated gas. The reference canister has been measured against the equilibrated gas, and the measured clumping anomaly has been subsequently assigned to the reference canister.

It is assumed that the temperature of the ice-water is well known, as the temperature-pressure relationship is very weak at atmospheric pressure ranges. Between a range of 1 and 10 bar absolute pressure, the melting point of ice

ΔDD	SE
236.84	2.80
231.41	4.15
231.18	2.63
Average	
232.48	1.67

Table 1: Direct calibration experiments performed at ice water temperature. The average of the ΔDD with it's respective standard error of the experiments is given, and its average and standard deviation

changes 0.08K. Normal atmospheric ranges of pressure are between 0.97 and 1.04 bar, causing temperature changes smaller than 0.01K, corresponding to ΔDD changes of 0.013‰.

The calibration experiments gave a lower clumping anomaly in the reference gas, than was assumed in the February experiments. The February measurement set indicated clumping anomaly near 240‰, instead of the calibrated 232.48‰ in May. It was possible to retroactively calibrate the reference canister of the February ice-water experiments, by inverting the calculations of δD and δDD. These experiments gave a clumping anomaly of the reference canister of 237.9 ± 1.7‰. However, note that this inverted calculation is performed on the average δD and δDD. If the calculation is performed on all individual measurements, the mean becomes $\Delta DD = 236.0 \pm 6.8$‰. Due to the larger number of available measurements, I assign the former clumping value to the reference gas over the February measurements.

It is important to note that, as the reference canister has been calibrated in two different ways, at two different times, they are used for their respective data-sets.

3 Theory

3.1 Partition function

In this section I explain out the theory required to calculated the expected clumping anomaly of molecular hydrogen. Consider the equilibrium reaction:

$$H_2 + D_2 \leftrightarrow 2HD \tag{20}$$

In any chemical reaction, the balance can be derived from the ratio of partition functions depending on the energy levels of the molecules. The partition function can be calculated if both the temperature, and if all energy levels of the system are known quantities, and is expressed as:

$$Q(T) = \Sigma_{i=0}^{\infty} g_i e^{\frac{-E_i}{k_B T}} \tag{21}$$

Where g_i denotes the degeneracy of state i, E_i the energy of that level, k_B the Boltzmann constant, and T the temperature in Kelvin. Energy can be decomposed into the sum of it's components, and this allows to simplify parts of this sum. Such an expression becomes:

$$\begin{aligned} Q(T) &= \Sigma_{i=0}^{\infty}\Sigma_{j=0}^{\infty} g_i \times g_j \times e^{\frac{-E_i}{k_B T}} \times e^{\frac{-E_i}{k_B T}} \\ &= \Sigma_{i=0}^{\infty} g_i e^{\frac{-E_i}{k_B T}} \times \Sigma_{j=0}^{\infty} g_j e^{\frac{-E_j}{k_B T}} \end{aligned} \tag{22}$$

Though this seems like a small step, this is helpful in evaluating the partition function. Any quantum mechanical system has energy levels depending on different quantum numbers, and this allows to evaluate on the separate numbers.

3.1.1 Electronic partition function

Lets start out by the most well known partition function of a quantum system, the electronic states. The partition function for such a system reads:

$$Q_{elec}(T) = \Sigma_{n=1}^{\infty} n^2 e^{\frac{-E_n}{k_B T}} \tag{23}$$

With the degeneracy of the system given by n^2. Consider in this case atomic hydrogen, for reasons which become clear at the end of this section. The energy levels of that system is given by:

$$E_n = \frac{\mu e^4}{8\epsilon_0 h^2}(1 - \frac{1}{n^2}) \text{ with } n \geqslant 1 \tag{24}$$

It is obvious that the energies of this system quickly approach its asymptotic value (the ionization energy), that part would make it easy in the evaluation of this partition function. However, the degeneracy is a diverging list, preventing us from directly evaluating this sum. So we need to have a justified reason to truncate this partition function at given n.

It is possible to find physical justification for this problem. Consider the expectation value for the radius of the electron around the nucleus:

$$r = \frac{n^2 h^2 \epsilon_0}{\pi \mu e^2} \tag{25}$$

with h denoting Planck's constant, μ the reduced mass of the protium-electron system, e the electron charge and ϵ_0 the vacuum permitivity. If this is evaluated for $n = 1$, one ends with a radius of $r = 0.53\,\text{Å}$. This seems reasonable within the confines of our experiment. Evaluate it for $n = 10$, and the radius becomes $r = 53\,\text{Å}$, still reasonable for this experiment.
Now if this is evaluated for large n (e.g. 10^5), the radius becomes $0.53\,\text{m}$, well outside the confines of quantum mechanics, or even the tube holding the hydrogen gas. Within this ever increasing radius, we find our justification to truncate the partition function at given n [6].
Let us evaluate this sum at the lowest temperature we will reach during this experiment, liquid nitrogen $77\,\text{K}$, for very large n:

$$\begin{aligned} Q(T = 77K) &= 1 + \Sigma_{n=2}^{10^5} n^2 e^{\frac{-E_n}{k_B T}} \\ &= 1 + 4 * e^{-9.1*10^6} + 9 * e^{-1.1*10^7} + ... \\ &\approx 1 \end{aligned} \tag{26}$$

The origin of this exercise is taken from [6], and checked with personal calculations. This gives us the justification needed to set the electronic partition function to 1, by truncating it at a reasonable value for the confinements in our experiments.

3.1.2 Vibrational partition function

For the vibrational partition function, two things have to be taken into account. First is the possible degeneracy of the system. Any molecular system has $3N$ possible displacements (3 for each of the atoms), of which 3 is equivalent to translation (e.g. all atoms moving uniformly in the positive x-direction), and for a linear molecule 2 correspond to rotation. This leaves 1 possible configuration for vibration.
The second is the energy of the vibrational states, given by:

$$E_j = (v + \frac{1}{2})\omega_e - \frac{1}{4}(1 + \frac{1}{2})^2 \chi_e \omega_e \tag{27}$$

With ω_e and χ_e are molecular constants, the first term of the right-hand side is the harmonic energy, and the second term the anharmonic correction. Hydrogen only has the first anharmonic correction, other molecules allow for higher order corrections.

3.1.3 Spin partition function

In the previous partition functions, the nature of the isotopologues was irrelevant for the derivation, as only molecular constants would differ between the

different compositions. However, when examining spin we need to account for the quantum-mechanical differences between protium and deuterium.
Protium behaves as a fermion (spin 1/2 particle) and deuterium as a boson (spin 1 particle). This has implications for the wave-functions of the molecular systems.
The Pauli-exclusion principle states that no two fermions may occupy the same quantum state simultaneously. This implies that the total wave-function for H_2 has to be anti-symmetrical.
To understand this, let us look at the wave-function:

$$\Psi = \tilde{\psi}_{spatial} \times \tilde{\phi}_{spin} \tag{28}$$

Where the spatial and spin wave functions can either be symmetrical or anti-symmetrical. As H_2 demands an anti-symmetrical wave function, so two possible configurations:

$$\Psi = \tilde{\psi}_{anti} \times \tilde{\phi}_{sym} \tag{29}$$

$$\Psi = \tilde{\psi}_{sym} \times \tilde{\phi}_{anti} \tag{30}$$

Now we examine the spin wave functions, the following combinations are possible for a two-electron system:

$$\phi_{sym} = \begin{cases} & |\uparrow\uparrow\rangle \\ S & \frac{1}{\sqrt{2}}(|\uparrow\downarrow\rangle + |\downarrow\uparrow\rangle) \\ & |\downarrow\downarrow\rangle \end{cases}$$

$$\phi_{anti} = \frac{1}{\sqrt{2}}(|\uparrow\downarrow\rangle - |\downarrow\uparrow\rangle)$$

Where $\uparrow$ denotes spin-up, and $\downarrow$ denotes spin-down. The solution to the spatial wave function determines the coupling with the spin wave function, to make the total wave function anti-symmetrical. Only the spatial symmetric solutions yield a bonding state with energies lower than the H_2^+ ion. Thus for the ground state, an anti-symmetric spin wave function is required, to have the total product to be anti-symmetric.
In the first excited state, the spatial wave function becomes anti-symmetrical, thus the spin wave function becomes symmetrical. In short, for $j = 0, 2, 4, ..$ we have the anti-symmetrical configurations for the spin wave function, for $j = 1, 3, ..$ the symmetrical configurations.
Now recall that deuterium behaves as a boson, and thus requires a symmetrical solution to the wave function. This yields 6 configurations for the symmetrical spin wave function, and 3 for the anti-symmetrical spin wave function. The ground state must be symmetrical (chapter 10.5 [4]).
These different states, combined with the requirement of the final wave function, yields nuclear statistical weights. For H_2 these are $\frac{1}{4}\big|_{j=even}$ and $\frac{3}{4}\big|_{j=odd}$, for D_2 $\frac{2}{3}\big|_{j=even}$ and $\frac{1}{3}\big|_{j=odd}$.

On top of the statistical weights introduced through the different wave functions, the energy levels are degenerate. This degeneracy is the same for all isotopologues, and is given by $(2j+1)$, where j is the spin energy level.

3.1.4 Translational partition function

The translational partition function describes the energy due to molecular movement. It can be derived through the quantum concentration of a gas. A generalized computation of the partition function is given by ([1]):

$$Q_{tra} = \int_0^\infty g(k) e^{\frac{-E(k)}{k_B T}} dk \tag{31}$$

where $g(k)$ denotes the density of states (analogous to the degeneracy used earlier), $E(k)$ the energy of a molecule with wave-vector k. This relation becomes:

$$\begin{aligned} E(k) &= \frac{\hbar^2 k^2}{2m} \\ Q_{tra} &= \int_0^\infty \frac{V k^2}{2\pi^2} e^{\frac{-\hbar^2 k^2}{2mk_B T}} dk \\ &= \frac{V}{\hbar^3} (\frac{mk_B T}{2\pi})^{3/2} \end{aligned} \tag{32}$$

3.1.5 Equilibrium constant

Having defined all the constituents of the partition function, this is now combined to the equilibrium constant. Recall the equilibrium reaction 20. Any chemical reaction of the form:

$$aA + bB \rightarrow cC + dD \tag{33}$$

where capital letters denote the chemical species, and the lowercase denote the number of molecules. The equilibrium constant of this reaction is given by ([1]):

$$\begin{aligned} K_{eq} &= \frac{Q_C^c Q_D^d}{Q_A^a Q_B^b} e^{\frac{-\Delta E_0}{k_B T}} \\ K_{eq,H_2} &= \frac{Q_{HD}^2}{Q_{H_2} Q_{D_2}} \end{aligned} \tag{34}$$

In an equilibrium reaction of isotopologues, ΔE_0 should be zero, and is considered to be so during this calculation. If the partition function were to be expanded in the form:

$$\begin{aligned} Q(E,T,m) =& Q_{tra}(T,m) \times Q_{elec}(E,T) \times \\ & Q_{vib}(E,T) \times Q_{spin}(E,T) \end{aligned}$$

To simplify this equation, consider the term on the right-hand-side in light of equation 34.

Translational partition functions: In the closed system, all constants and variables are equal of equation 32, apart from the mass. Consequently, only the ratio of masses is retained, and this becomes:

$$R_{tra} = (\frac{3^2}{2 * 4})^{(3/2)} = (\frac{9}{8})^{(3/2)}$$

Electronic partition function: All of the electronic partition functions are set to 1, with the physical justification given in section 3.1.1

Vibrational and spin partition function: The energy levels of all isotopologues are not the same, so this part is retained as depending on the different energy levels. For this work, the sums have been contracted, as use has been made of the *ab inito* calculations of Komasa *et al* [5] and Przybytek *et al.* [9] The partition sums have been evaluated with the energy levels from those calculations.
These are the explicit energy levels of the ro- and vibrational spectra, for both quantum number j and v. This approach combines the spin- and vibrational partition functions.
Only the degeneracy of the spin partition function has to be taken into account, as the degeneracy of the vibrational partition function is 1.

3.2 Spin isomer effect

During this work, it has been assumed that the spin isomer distribution resets during isotopic re-equilibration. Hydrogen gas in thermodynamic equilibrium has a fixed distribution between the ortho- and para hydrogen. This distribution can easily be derived from the partition function, by calculating the ortho- and para states separately.
To split this, we seperate the partition sum in odd and even values for the quantum number j. This allows us to evaluate the partition function for only ortho states. The ratio of this sum over the full partition function gives the probability of finding a molecule in the ortho-state.
In figure 3 the thermodynamic ratio of ortho:para states is shown, depending on temperature. At high temperatures, this ratio remains constant. But at low temperatures, the lowest energy states become more important in the partition function, giving more weight to the even states ($j = 0, 2, ..$).
This also allows us to examine the extremes of the system. Suppose only ortho or para states are allowed within this system. These results are shown in figure 4. There is one final step to this calculation, that is to fix the spin distribution over the whole temperature range.
This calculation started out from the thought experiment: Suppose on re-equilibration of isotopologues, the spin distribution is not altered. That is, for H_2, that the distribution remains 3:1, even for low temperatures. To have this distribution, one would require that $\frac{Q_{ortho}}{Q} = \frac{1}{3}$ for all temperatures (and

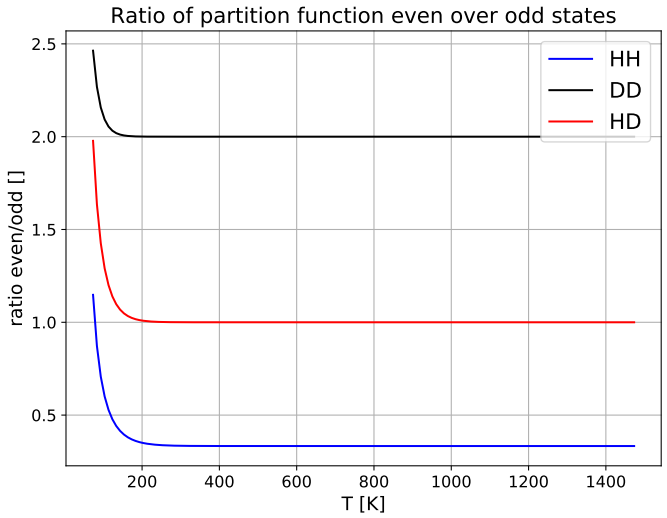

Figure 3: The spin distribution of the isomers, as defined as even diveded by the odd states. This is the corresponds to the probability to have a hydrogen molecule in the even or odd state. E.g. at high temperature, a H_2 molecule has a 25% chance to be in the even state.

similar results for the other isotopologues). This imposes an unequal mixture of gases, but I did not manage to get the mathematics around this solved.
The strong difference in the ortho- and para calculations (figure 5, when compared with all quantum states allowed can be explained by the nuclear statistical weights used. In this computation, I set the respective weights to 0, and kept the other weights the same.

It is very important to note that the HD isotopologue has no distinction in these states, as it has no ortho or para states. In the calculations for the ortho and para results, both statistical weights are kept at 1. Whereas in the computation for even or odd states of j, these have been altered, as specific states were explicitly disallowed.

3.3 Mixing of gases

Though the clumping anomaly is a temperature dependent function for equilibrated gases, it is possible to induce an anomaly by mixing gases of different isotopic composition, even if the gases are in the same equilibrium.

When mixing two gases, the ratio of isotopologues becomes a linear combi-

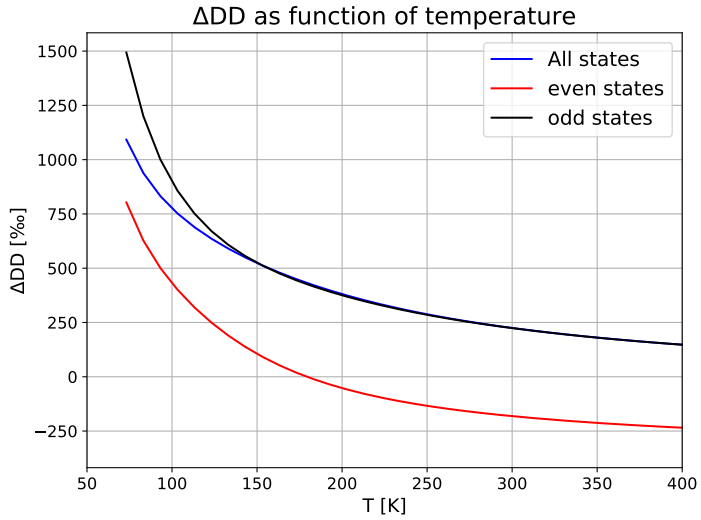

Figure 4: Δ DD of thermodynamic equilibrium, $j = odd$ or $j = even$ states. The even or odd are the extremes of the possibilities, and are shown to indicate that at low temperatures, this would induce a strong difference in ΔDD.

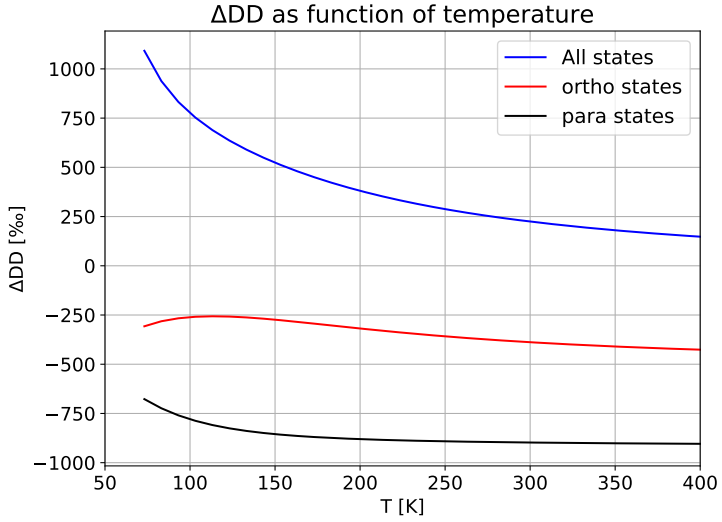

Figure 5: ΔDD where only para or ortho hydrogen/deuterium is considered. As HD makes no distinction between these states, all states have been allowed in this calculation

nation of the mixture, e.g.:

$$R_{HD} = (1 - \alpha) \times R_{HD,1} + \alpha \times R_{HD,2} \text{ with } 0 \leqslant \alpha \leqslant 1 \tag{35}$$

Using this relation, the clumping anomaly can be computed from the initial ratios of the mixed gases. At the start of experiments, the clumping anomaly can be measured, or assumed. From this, and the δD-value of the gas, the expected clumping anomaly of a mixed gas is determined through:

$$\begin{aligned}
\delta DD &= \frac{\frac{\Delta DD_i}{1000} + 1}{R_D^2} \\
R_{mixed} &= (1 - \alpha) \times R_{gas1} + \alpha \times R_{gas2} \\
\Delta DD_f &= (\frac{R_{DD}}{R_D^2} - 1) \times 1000
\end{aligned}$$

4 Experimental results

4.1 No equilibration without catalyst

To determine the equilibrated clumping anomaly, it is essential that the hydrogen gas does not equilibrate quickly at any other point than the catalyst. No cooling experiments were performed in tubes without (activated) catalyst, experiments were performed using inactive Cr_2O_3. In this system, H_2 could re-equilibrate on the quartz, glass, Cr_2O_3 or Teflon Young valve.

Two different fillings of the tubes were performed, each sampled multiple times with increasing time in the nitrogen bath ($3 \leqslant t \leqslant 24h$). An extra datapoint has been included, which was inactive Cr_2O_3, at room temperature for 15 minutes before sampling the gas, to fix the $(0, 0)$ point in the graph. The results are shown in figure 6

No signal in δD and δDD was expected of the inactive Cr_2O_3, but the experimental results did show some form of interaction between the gas and the surfaces. The relation between the isotopic signatures was a $1:2$ relation, indicating mass dependent fractionation.

Mass dependent fractionation is induced due to the absolute mass differences between the isotopologues. The linearized mass dependent fractionation reads:

$$\delta D \approx 0.5 \times \delta DD \tag{36}$$

In figure 6 we see this $1:2$ relation of the isotope values. Combined with the gas still measuring the assigned clumped value of the gas, I conclude that no re-equilibration has occurred with all of the possible catalytic surfaces.

As there is a clear signal in the isotopic values of the gas, this seems to indicate a surface effect. It is suspected that hydrogen either absorbs to the Cr_2O_3 or the quartz surface, and does not undergo catalytic isotope exchange while in this absorbed state.

4.2 Cr_2O_3 experiments

Experiments were performed using different tubes with Cr_2O_3, with the traditional cooling baths (see section 2.3). Different procedures were used to activate the catalyst, and results are shown in figure 7. Only IMAU H2 line gas has been used for these experiments.

4.2.1 Cr_{O3} at liquid nitrogen

High temperature experiments with this catalyst agree with theory, and shows that the Cr_2O_3 catalyst does re-equilibrate hydrogen. Low temperature exper-

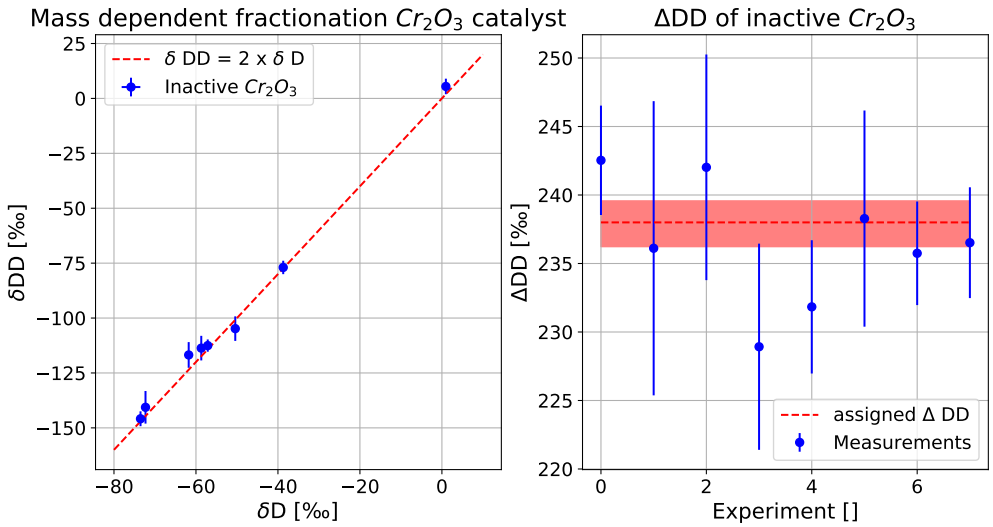

Figure 6: δDD vs δD of cooling experiments. Datapoint near (0,0) was inactive Cr_2O_3 at room temperature. The mass dependent fractionation is clearly visible, and the room temperature sample is included to extend the line. The assigned clumping anomaly was 238.9‰, all measured clumping anomalies cluster around this value indicating no equilibration.

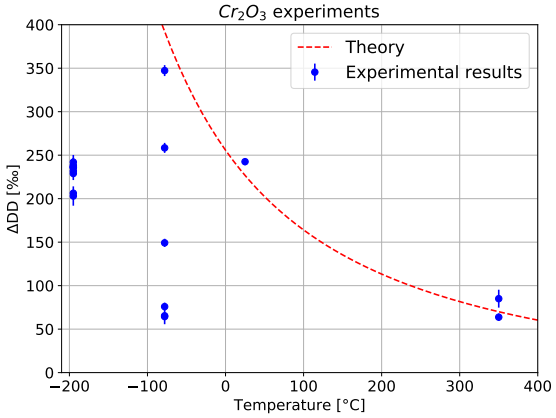

Figure 7: Overview of the Cr_2O_3 experiments. Temperature indicated is the assumed equilibrium temperature (either of the oven, or the cooling bath), temperature set at 25°C is taken at room temperature. For some results the uncertainty is too small to be visible. Experiments do not seem to reset clumping, except for heating, and 1 set of dry ice experiments.

iments show ambiguous results. For liquid nitrogen experiments, two different tubes were used with different activation procedures and fillings, equilibrium times between 3 and 32 hours.
None of the experiments at liquid nitrogen show indication of re-equilibration of the isotopologues. One of the fillings measured had catalyst which did re-equilibration at dry ice temperatures, and remained under vacuum or hydrogen atmosphere between the experiments. The catalyst should be active during the liquid nitrogen experiment.
All experiments conducted at this temperature measured clumping anomaly close to the assigned clumping anomaly of the gas, instead of the expected clumping anomaly ($\Delta DD|_{T=77K} = 1024.94‰$).
Taking the non-interacting nature into account we conclude that the Cr_2O_3 does not act as a catalyst for reaction 20 at liquid nitrogen, with the activation procedures used during this work.

4.2.2 Cr_2O_3 at dry ice

Dry ice + ethanol ($T = -78°C$) experiments had dual results. Depending on the activation procedure used, it either did or did not alter the clumping anomaly of the original gas.
Two tubes were used for the dry ice experiments, each measured with 1 filling. One of these fillings did show altering of the clumping anomaly, with increased equilibrium time. Though this indicates that Cr_2O_3 does work at dry ice temperatures, the required equilibrium time makes this an unfavorable catalyst for this research. Results are shown in table 2
The expected clumping anomaly is $\Delta DD|_{T=195K} = 392.47‰$. Even after 19.3 hours of equilibration time, the activated Cr_2O_3 did not reach expected equilibrium. The second of these fillings do no show re-equilibration after bringing to dry ice temperature. Note that this had a different activation procedure, which did not seem to activate this catalyst for low temperature experiments. Results of this filling agree with the expected clumping anomaly of filling temperature ($\Delta DD|_{T=623K} = 70.03‰$)

4.2.3 Cr_2O_3 conclusion

Only two dedicated heating experiments are conducted with this catalyst. Note that this means that the gas was sampled at the heated temperature ($T = 350°C$). Results are given in table 3.
The first experiment is not in equilibrium, but does seem to approach it. This can be due to slow reaction rate with this catalyst. The second experiment seems to agree with theory.
Due to inactivity at liquid nitrogen temperatures, ambiguous and slow results at dry ice temperatures, I conclude that the Cr_2O_3 catalyst in this form, with these activation procedures, is unsuited for the purposes of this research.

Time (hours)	ΔDD(‰)	SE	N
2.32	151.16	4.68	20
10.37	260.47	5.77	16
19.32	349.53	6.29	20
30.66	66.25	4.09	16
45.66	67.15	9.69	8
48	77.71	4.6	5

Table 2: Overview of the dry ice experiments with Cr_2O_3. The first three experiments were a different tube than the latter three. A different treatment of the catalyst activation may explain the difference in behavior.

Time (hours)	ΔDD(‰)	SE	N
0.42	86.86	10.31	8
21.5	65.57	4.26	14

Table 3: Heating experiments (350°C) with Cr_2O_3. Both experiments were the same tube and same filling, only sampling time differs. Specific tube is the same as the working dry ice Cr_2O_3 experiments.

4.3 Platinum on carbon catalyst

4.3.1 Heating experiments

Heating experiments were conducted in two sets, February and May. In the February set, results were ambiguous, but indicated that it was in equilibrium. Some samples taken were to investigate the initial state of the gas, and was not fully in equilibrium. Three experiments were conducted dedicated to heating, with equilibrium times between 5 and 22.5 hours.
During the 5 hours experiment, the isotopic values in δD and δDD seem to undergo a drift over the experiment, yielding a high clumping anomaly. The cause of this issue is uncertain. Later experiments performed on new sampling of the same gas did not undergo this drift, and yielded results more in line with theory.
Cr_2O_3 was used in some heating experiments, but only 1 dedicated. This was performed at 350°C, and seems to underestimate the clumping anomaly at that temperature.

During the experiment set of May, two conditions were altered. The catalysts were placed in new tubes. And use was made of the platinum mesh catalyst. Heating experiments were conducted using both catalyst (separate tubes), at two temperatures (150°C for Pt mesh and 300°C for both) to match the developed experimental scale with previous results by Popa *et al.*[8].
These experiments gave higher clumping anomaly than theoretical predictions, and is not consistent with experiments conducted in February.

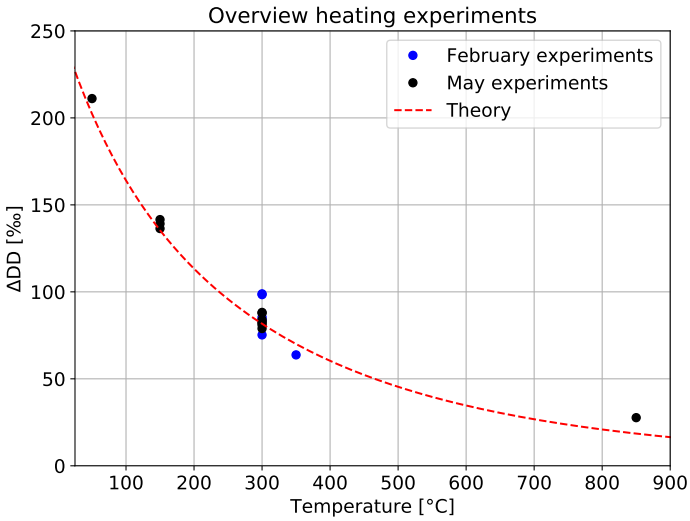

Figure 8: Overview of the performed heating experiments. May experiments seem to overestimate the clumping anomaly at temperatures

Investigated root causes of this issue were:
(1) Temperature at the catalyst. The temperature was probed using a thermocouple in the oven. At the bottom of the tube, a temperature difference was present of $15K$ between the bottom and the assigned temperature. A few centimeters inside the heating oven, assigned temperature was reached. This part is bridged using a small ceramic tube, raising the heating tube to the correctly heated part of the oven.
(2) Out-gassing of the catalyst/tube. The platinum mesh catalyst was heated to 850°C and evacuated, to condition the catalyst and out-gas the system. Experiments were performed at 300°C before and after this heating, and gave similar results.
(3) Catalyst dependence. Experiments were performed at the same temperature using both catalysts. Both experiment sets gave similar results, thus this issue is independent on used catalyst.
(4) Temperature gradient. To investigate if this is due to temperature gradient, an experiment was performed with the oven heated to 50°C, to reduce any possible gradient induced due to the exposed quartz tube. Anomalous high ΔDD was measured in this experiment.

None of the heating experiments conducted in the May set agree with theory, or with previous experimental results using the same reference gas used in February. Multiple possible causes have been investigated, but no satisfying solution has been found. It remains unclear why experiments conducted using

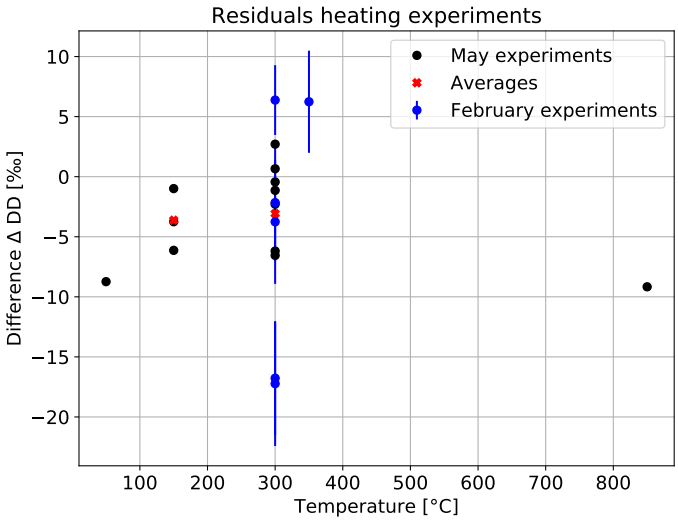

Figure 9: Residuals of the heating experiments. The error bars for the May experiment set are not shown to keep the figure readable. The experiments overestimate the clumping anomaly in the May experiment set.

the heating oven disagree with previous results, while cooling experiments agree with previous results.

The residuals are shown in figure 9. The May experiment set overestimates the clumping anomaly, where the February experiment set is ambiguous on the results due to the low number of data-points gathered in that set.

4.3.2 Cooling experiments

Cooling experiments were performed in two different periods, the results of which are shown in figure 10. The results are given without error bars to keep the figure readable, but the standard errors of the measurements are in the order 2-4 ‰. The results initially seem to agree with the theoretical calculation, but this is due to the scale. The residuals of this are shown in figure 11

Liquid nitrogen:
The liquid nitrogen experiments had large variability in the results. The outlying result (with residual ∼23‰was performed with the enriched NAT360 gas, but a second experiment using this gas gave results comparable to the IMAU line H2. It cannot be insufficient equilibration time, as these samples equilibrated longer than 12h.
The results of IMAU H2 were very consistent. 4 Experiments were performed at this temperature, all results were within the standard error of other results. All

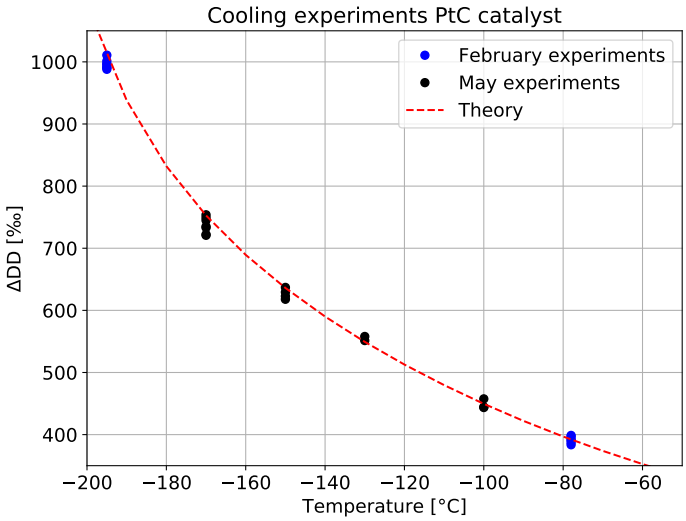

Figure 10: Overview of the cooling experiments conducted. Error bars have not been plotted to keep the figure readable, but are of order 2-5‰. The May experiment set used the copper cooling device.

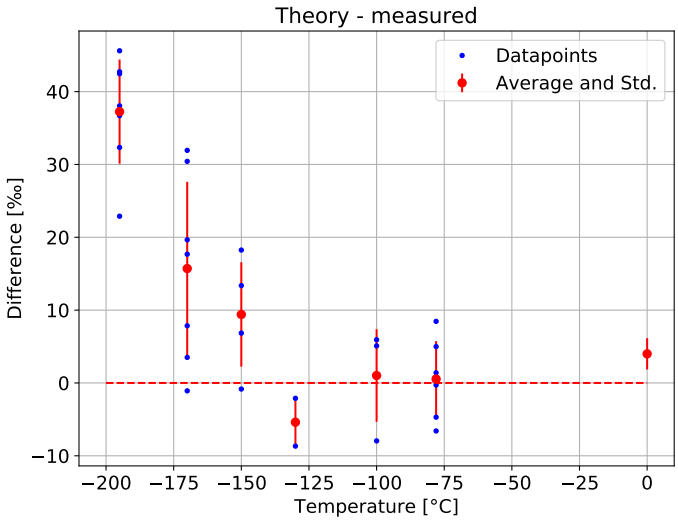

Figure 11: All cooling experiments with PtC performed. The residuals if theory minus measured clumping anomaly. Positive residuals give that theory overestimates the clumping anomaly.

experiments conducted at this temperature underestimate the clumping compared to theoretical predictions.
The residual is (with the outlying result included) 37.25 ± 7.15‰, with the outlying result removed the residual becomes: 39.64 ± 4.43‰

$-170°$**C**

The results are obtained over 4 different fillings, all with NAT360 gas. The two results with high ΔDD residual are from the same sampling of the gas, equilibrated for 3 hours, measured at different pressures. The time used to equilibrate the gas should be sufficient, as an earlier sample seemed to be equilibrated after 2 hours. It is unclear why this sample is underestimating the clumping anomaly, while the other samples yield a larger clumping anomaly.
As with the liquid nitrogen experiments, experimental results underestimate the clumping anomaly. If the two outliers are removed, the residual becomes 9.52 ± 8.0‰, with the outliers included the residual is 15.71 ± 11.90‰

$-150°$**C**

Results are obtained from 4 fillings, spaced with other temperature experiments sampled from the same tube. Cooling times between 3 and 4.5 hours have been used for these experiments. Three of the experiments seem to underestimate the clumping, where one experiment agrees with the theory. This experiment was brought to $-170°$C before equilibrating at $-150°$C.
As this sample has equilibrated for 4 hours at $-150°$C, I assume it to be in equilibrium. I conclude that the results overestimate the clumping anomaly. The residual of this set is 9.40 ± 7.16‰

$-130°$**C**

Due to time constraints, only two experiments were performed at $-130°$C. Both experiments were new fillings, and have not been sampled at different temperatures beforehand, and had 4 hours to equilibrate. These results seem to overestimate the clumping anomaly at the given temperature. The residual of this set is -5.39 ± 3.28‰

$-100°$**C**

Results are of three different fillings, all with cooling time of more than 4 hours. Samples have been taken from fresh and earlier sampled tubes. The two datapoints near each-other were of a new filling, and a previously sampled tube. There seems to be no relation between ΔDD and previous samplings of the tubes.
If the negative residual result is treated as an outlier, and removed, the residual differs $+5.5 \pm 0.42$‰ from theory, with the outlier included the residual is $+1.02 \pm 6.36$‰.
The former result has only two datapoints, and the third one would arbitrarily be treated as an outlier. I assign the latter residual to this data-set.

Dry ice + ethanol

In the February data-set, many experiments were conducted at the dry-ice + ethanol temperature. Though there seems to be variability in this set, the average of these results seem to agree with the theoretical calculations. The residual

of this data-set is 0.54 ± 5.20‰.

possible explanations:
Almost all results seem to underestimate the clumping anomaly, apart from -130°C or dry ice + ethanol. It is important to remember that these results are obtained in two different periods. There may be a couple of explanations for the measured clumping anomaly.

1: The calibration of the working gas in the May experiment set is wrong. If the calibration performed in May underestimates the clumping anomaly of the reference gas, all results underestimate the clumping anomaly by roughly the same number. But this does not explain two observed things: The increasing deviation with decreasing temperature; And it does not explain the -130°C temperature result, as this would differ more from theory.

2: A different temperature at the catalyst than assumed. Between the different experiment sets, the cooling device insulated the tubes more, only exposing a small part of the valve to the atmosphere. This does not explain the results of dry ice, as a temperature gradient would be expected in that situation, nor does it explain the -130°C or -100°C results. Only the -100°C results would agree with the existence of the temperature gradient is the negative residual result is treated as an anomaly and removed from the data-set.
This can be investigated further by examining the effects of a shift in temperature. Suppose the temperature at the catalyst is 2°C higher than expected, the residuals of this thought experiment are shown in figure 12. Though the shift of 2°C is completely arbitrary, and each temperature should have its own shift, this does explain the behaviour at different temperatures.
I deem it unlikely that a temperature shift at the catalyst is the explanation for the difference observed in the experiments, as this would not be consistent over the data-sets, and the insulation of the tube seems to have no effect.

4.3.3 Hysteresis experiments

To show that the initial state of the gas is not determining for the final state, hysteresis experiments were performed. As the ice-experiments were retro-actively used for calibration of the reference gas, results of these experiments at ice-water temperatures are not shown here.
The results obtained with the hysteresis experiments are not distinguishable from the cooling experiments at dry ice temperatures (figure 13. This shows that the clumping anomaly is independent of the previous states.
This is also implicitly proven by using the enriched NAT360 gas, what has an initial ΔDD of ~ 26000‰.

In figure 13 results of both gases are explicitly shown, and the clumping anomaly does not depend on the different gas used. From this I conclude that the bulk isotopic composition does not determine the clumping anomaly of equi-

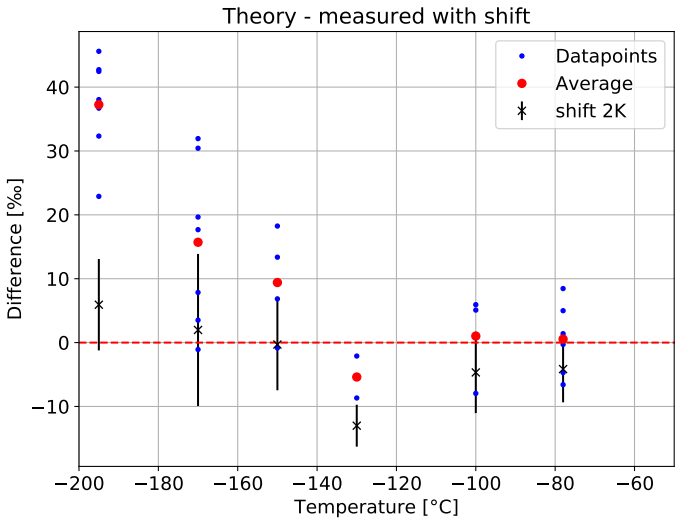

Figure 12: The residuals of the cooling experiments. In red the averages before a shift in temperature is applied, in black the difference with theory where the theory is calculation at 2°C higher than assumed.The very low temperatures seem to agree better with the theory, but the higher temperature results seem to underestimate the clumping.

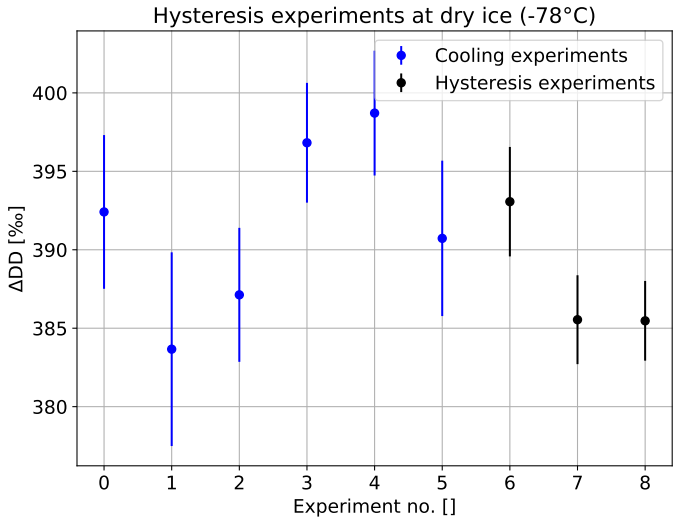

Figure 13: Overview of the hysteresis experiments. The datapoints in blue are from the February data-set, with both NAT360 and IMAU H2 equilibrated at dry ice temperatures. Black data-points were brought to liquid nitrogen temperatures for more than 4 hours to equilibrate, before equilibrating at dry ice temperature.

librated gas. This can also be shown using liquid nitrogen results, but this data-set had more spread (see figure 11)

4.4 Mixing experiments

To validate the measurements, mixing experiments were performed. For these experiments, NAT360 and IMAU H2 line gas were equilibrated at ice-water temperature, and measured at the start of the experiment to determine the isotopic composition and initial clumping anomaly.

The mixture of the gases is determined by the δD of the measured gas, with the initial measurements used as the boundary conditions for this. The gas used to dilute the sample bellow (mixing it) is stored in the Ultra. At the start of the mixing experiments, NAT360 equilibrated at ice water was stored for 12 days in a bellow of the Ultra. Measurement of this gas indicated no re-equilibration of the gas.

The mixing experiments were performed in two sets, each set starting out

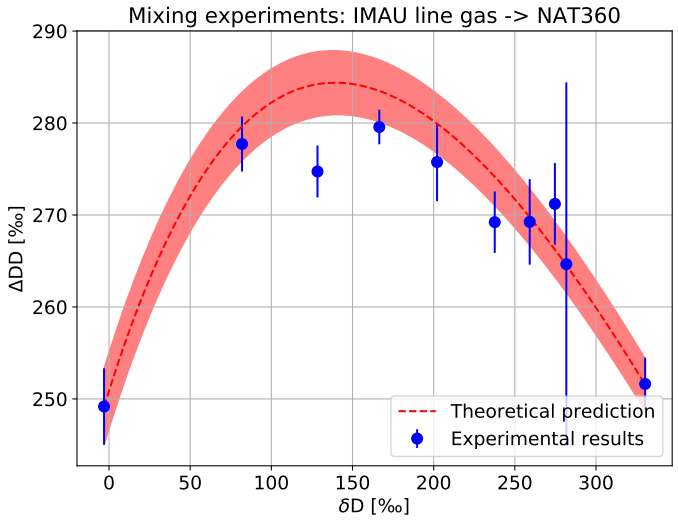

Figure 14: Overview of the first mixing experiment. The shaded area is deceptive, as it takes the lower and upper bound of both initial states to compute it. These bounds are determined as 1 standard error of the initial measurements. Initial gas was line gas ($\delta D = -150‰$), diluted with NAT360 ($\delta D = +205‰$)

with a different gas. The δD of the gas is given by:

$$\delta D_{sample} = (1 - \alpha) \times \delta D_{gas1} + \alpha \times \delta D_{gas2} \text{ with } 0 \leqslant \alpha \leqslant 1 \tag{37}$$

From this relation, and the known δD of all gases, the mixing fraction between gas 1 and 2 can be determined.

In the first mixing experiment set, the measurements seem to underestimate the expected clumping, whereas in the second experiment set the results seem to overestimate it. However both seem to hold a pattern within their respective dataset, indicating that the initial determination of the gases may explain the deviation, shifting the data towards one side of the shaded area.
Both datasets have outliers, these may be due to the relatively short measurements performed when mixing the gases. It was chosen not to perform long experiments, to reduce the gas depletion of the bellow and thus increase the number of experiments able to be performed. This clumping anomaly measured here is created by the mixture of the gases, and is thus independent of the temperature at the catalyst, and the created anomaly is independent of the clumping anomaly of the gases. These results show that the measured clumping anomalies in the cryogenic region are not an artifact of the machine, as these results follow the prediction well (especially for the second mixing set).

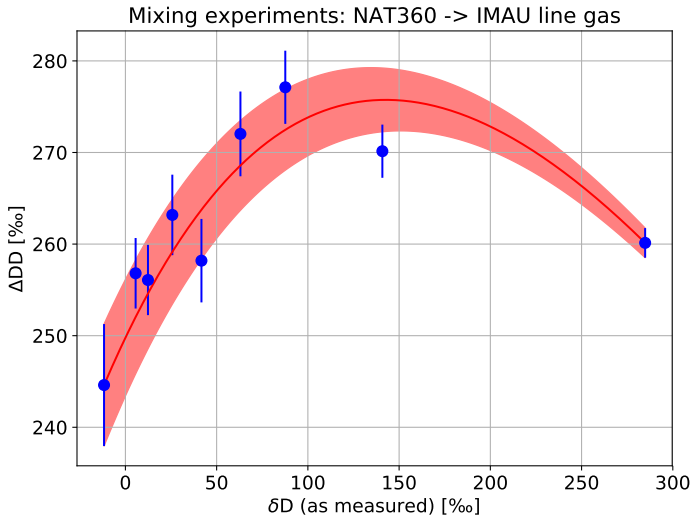

Figure 15: Overview of the second set of mixing experiments. The experiments started out with NAT360 gas. The shaded area is the expected clumping with $\pm\sigma_{SE}$ of the initial determinations of the gases.

4.5 Stability of measurements

Over the experiments, the obtained standard error was compared to expected standard error from counting statistics. In the February data-set, the ratio of experimental standard error divided by the expected standard error was between 0.5 and 1.5 when IMAU H2 line gas was used. This ratio became larger than 2 when measuring the enriched NAT360 gas. It is unclear why the standard error of the NAT360 gas in February was higher than the measurements of line gas. In the may data-set, most measurements were performed with NAT360, and had a ratio between 0.5 and 1.5, with some outliers. The stability of the system was comparable with the measurements performed in February. In the May data-set, the stability of NAT360 and IMAU H2 line gas were similar.

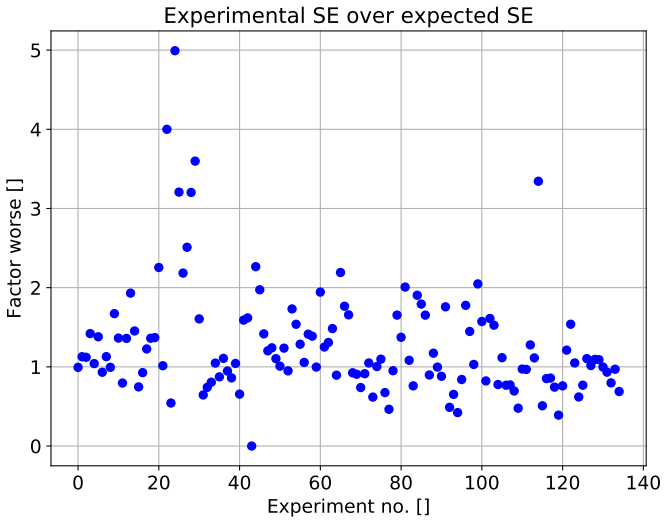

Figure 16: Overview of the ratio of experimental standard error over the expected standard error. High values near experiment no. 24 were performed with the enriched NAT360 gas. The outlier near no. 115 only had 3 data-points, resulting in a large standard error.

5 Discussion

5.1 Antoine equation

During the experiments, a cooling bath has been used to fix the temperature at the catalyst. It was assumed that the temperature of such a bath was static. During the data analysis, large variability was observed in the liquid nitrogen range, less in dry ice range, and little in ice-water range.

This could indicate that either the temperature at the catalyst was wrong, or that the samples were outside of equilibrium. As the different reaction times and the variability show no pattern (e.g. more reaction time shifts the result closer to the equilibrium), the former of the two assumptions seems more likely.

In a discussion with *Christof Janssen* he pointed out that the temperature of liquid nitrogen is a pressure dependent function. As no dedicated pressure log was maintained during the conduction of the experiments, and no temperature sensor was used in combination with the cooling bath, we rely on other logs.
To determine the pressure-temperature relation, the semi-emperical Antoine

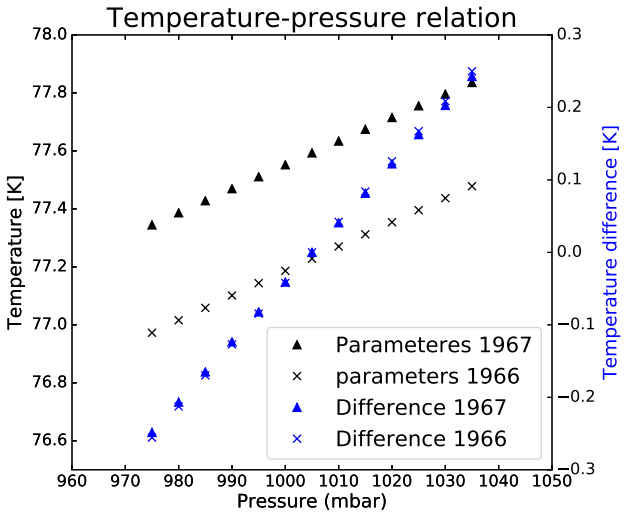

Figure 17: The pressure-temperature relation for two sets of parameters. On the left axis the absolute temperature with the parameters, on the right axis the temperature difference between pressure p_i and 1005 mbar.

equation is used. It is rewritten in the form:

$$T = \frac{B}{A - {}^{10}log(p)} - C \tag{38}$$

With A, B and C being molecular constants, and p the pressure in bar. This equation is dedicated to a single-molecular system, e.g. liquid-gas N_2 equilibrium. Our cooling bath consists of pure liquid N_2, evaporating during the experiment. Air already consists of 79% N_2, and this evaporating nitrogen shifts this even further, allowing us to approximate this as a pure N_2 gas.

Multiple different sets of molecular constants have been determined ([2], [7]). Though all yield different absolute temperatures, the temperature differences are comparable.

To determine the pressure differences, consider that the Dewar is exposed to the atmosphere through the hole at the cap. This implies that the pressure at the liquid-gas interface cannot deviate strongly from the atmospheric pressure. A pressure log exists over the month of februari through the H_2-isotope system. In figure 18 this is shown. The daily variations seem small, and no differences between day-night can clearly be seen. The pressure in the laboratory is dominated by the meso-scale weather system.

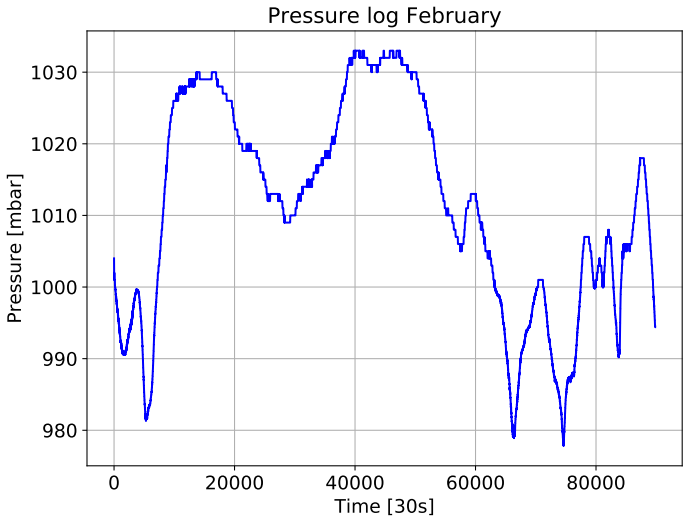

Figure 18: Pressure log over Februari. Y-axis pressure in bar, x-axis dimensionless time unit. 1 hour is approximately 120 dimensionless time units. The system is dominated by the meso-scale weather system, as seen by the timescale of the pressure variations.

To investigate the effect on the ΔDD, the results the calculation are shown with the temperature difference induced due to the pressure variations shown in figure 18. The deviations observed between the theory and the experimental results cannot be explained by the difference in temperature of the cooling bath. Error bars have not been plotted to keep the figure readable.

To match the results with the theoretical predictions, a temperature shift of approximately 1.5K would be required. However, with the atmospheric ranges, only a shift of $\pm 0.25K$ can be expected. It is entirely likely that the temperature of liquid nitrogen will shift a little over the time of the experiments, as this will be determined by the atmospheric pressure, but is is unlikely that this can explain the differences observed between theoretical prediction and experimental results.

5.2 Possible explanations

The deviation in clumping anomaly can be explained with different causes:
With the cooling experiments, the temperature at the catalyst is higher than the assumed temperature. This does not hold for all the temperatures, making this an unlikely cause.

The assumed temperature is wrong. With the liquid nitrogen bath, a change of a few permil can be explained by the temperature-pressure relation of liquid

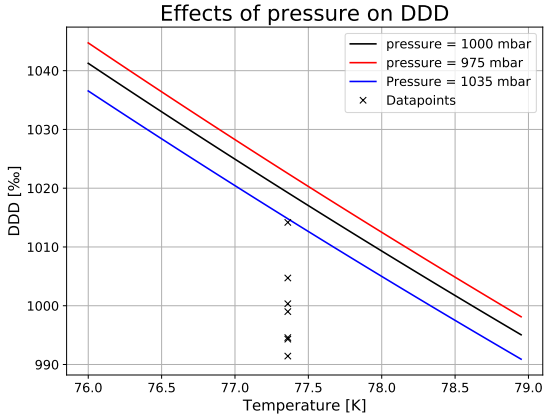

Figure 19: Pressure induced temperature shift at 975 mbar and 1035 mbar, with 1000 mbar as reference point. Datapoints are plotted at the temperature of liquid nitrogen, as assumed earlier in this work (-195.79 . The different lines now represent an uncertainty range.

nitrogen, but this does not hold for the use of the cooling device. This device uses a thermocouple to measure the temperature of the copper at catalyst height, and maintains this by use of heating wires, making a change in temperature very unlikely.

The reference gas is not properly calibrated. The heating experiments seem to overestimate the clumping anomaly, where (most of) the cooling experiments underestimate the clumping anomaly. This can be in part explained by a wrong calibration value of the reference gas. However, this would not be fully consistent in the for all cooling experiments. Second, this would only be a small change, of the order of 2‰, not enough to explain the observed differences.

The bias-correction is wrong. During the May experiment set, data was corrected for a bias in δD and δDD. As the δDD signal had more noise, this could not be determined between measurements. for δDD the correction was calculated by the average over all zero enrichment measurements. However, this correction is also applied to the calibration of the reference gas in the May data-set, making this an unlikely cause of the errors.

6 Conclusions and outlook

6.1 Conclusions

In this work, I determined the clumping anomaly of molecular hydrogen in the cryogenic region, and compared the results to theoretical predictions. In the region between $-196°C$ and $-150°C$ the experimental results underestimate the clumping when compared to theoretical predictions.
At $-130°C$ the experimental results overestimate the clumping anomaly, and at $-100°C$ and $-78°C$ the results agree with theoretical predictions.
I do not exclude the possibility that results obtained at $-130°C$ are outliers. The obtained results seem to agree with theory down to $-100°C$, and start deviating from theory below that temperature

A temperature difference at the catalyst may explain the former experiments, but does not explain the latter temperatures. For liquid nitrogen temperatures, a small change may be explained by the temperature of the cooling bath, but this does not explain the full difference observed.

Mixing experiments have been conducted to independently create a clumping anomaly, regardless of the temperature at the catalyst. The first set of experiments underestimates the clumping, the second set agrees with predictions. The former result can be explained by a measurement error in the initial determinations.
From these experiments I conclude that the clumping anomaly of a gas can be well measured, and that the results obtained with the cooling experiments are not artifacts of the machine.

By conducting hysteresis experiments, it is shown that the clumping anomaly of the gas does not depend on the previous clumping anomaly of the gas. This is also implicitly proven by the use of an enriched anomalous gas.

By the use of two gases, differing strongly in isotopic composition, it is shown that the clumping anomaly is independent on the bulk isotopic composition of the gas.

The conducted heating experiments, to match the results with previous work ([8]), overestimated the clumping anomaly. This may be explained by an error in the calibration of the reference gas.

6.2 Outlook

During this work, it has not been established if the measured clumping anomaly is independent of the catalyst used. Only the platinum nanoparticles on carbon were used for the cooling experiments due to time constraints. It should be

investigated if the catalyst has effect on the measured clumping anomaly.

The temperature at the catalyst is an assumed quantity during this work, but never been able to directly measure it. To exclude the possibility of a temperature difference at the catalyst, due to a temperature gradient. To eliminate this cause, experiments should be conducted with large cooled volume, and small volume exposed to atmospheric temperatures. This should reduce the temperature gradient, and fix the temperature at the catalyst better.

Few heating experiments were conducted in this work with the platinum nanoparticles on carbon catalyst. To match the obtained results with previous experimental results, more experiments are required.

Current measurements show interesting behaviour near $-130°$C, where experiments seem to overestimate the clumping anomaly, and lower temperatures underestimate the clumping anomaly. These results may be outliers. This temperature range ($-150°$ to $-100°$) would be interesting to investigate further.

Other present gases may interact in the source, changing the isotopic composition of the gases. A small amount of N_2 was present in the reference canister. It is interesting to investigate the effets of contaminants on the measured clumping anomaly.

7 Acknowledgement

During this research, I recieved help from three different people which I would like to thank very much.
In the start of this work, I was faced with the issue of catalytic equilibration of molecular hydrogen. I would like to thank Petra de Jongh and Peter Ngene of the chemistry department of Utrecht University for thinking with us to solve the problem of catalytic equilibration of molecular hydrogen at cryogenic temperatures, and supplying us with the catalysts required to conduct these experiments. Without Peter and Petra, I would have been unable to conduct these experiments, with catalytic equilibration at cryogenic temperatures.
I would like to thank Christof Janssen of the French National Centre for Scientific Research for helping me in understanding the partition function of molecular hydrogen, and helping me find the errors in the calculations I performed. Furthermore I'd like to thank him for the help during examination of the February data-set, and pointing me to possible origins of possible deviations from theory (e.g. the temperature of liquid nitrogen). Without Christof I would have not considered certain possible errors with the experimental results, and would not have found the errors in my theoretical calculations.

A Cooling device

The cooling device has been created to reach temperatures ordinarily not stable using traditional cooling baths. This device is cooled using liquid nitrogen, all-though other coolants are possible for higher temperatures. Without the heating wires wrapped around the copper cylinder, temperatures of $-190°\mathrm{C}$ can be maintained.
The device consists of:

- Hollow copper cylinder closed at the bottom
- 4 copper strips, $5 \times 2 \times 200\ mm$ $(w \times d \times h)$
- Copper pin (remove-able) at the bottom, $6 \times 100\ mm$ $(d \times h)$

The copper strips and pin are submerged in coolant, cooling the cylinder through thermal conduction. The copper pin is fixed at the bottom of the copper cylinder, conducting heat to the bottom of the tube. The copper strips are connected at 100mm height of the copper cylinder, conducting heat to that point. Extra surface contact has been made between the strips and the copper cylinder at that point, to increase the thermal conduction.
The heating wire is wrapped around the copper cylinder, and the temperature is probed using a thermocouple. This thermocouple is inserted into a drilled hole near the bottom of the copper cylinder, to probe the temperature of the copper cylinder near the bottom of the tube. The heating wire maintains the temperature at a set point. The device is insulated, to reduce heat exchange with the atmosphere.

References

[1] Stephen J Blundell and Katherine M Blundell. *Concepts in thermal physics*. OUP Oxford, 2009.

[2] Merardo P Edejer and George Thodos. Vapor pressures of liquid nitrogen between the triple and critical points. *Journal of Chemical and Engineering Data*, 12(2):206–209, 1967.

[3] Austin J. Gould. The inter-relations of hydrogen and deuterium molecules. *Journal of chemical physics*, 1(2):362 – 373, 1934.

[4] Mool C Gupta. *Statistical thermodynamics*. New Age International, 2007.

[5] Jacek Komasa, Konrad Piszczatowski, Grzegorz Łach, Michał Przybytek, Bogumił Jeziorski, and Krzysztof Pachucki. Quantum electrodynamics effects in rovibrational spectra of molecular hydrogen. *Journal of chemical theory and computation*, 7(10):3105–3115, 2011.

[6] EN Miranda. A paradox in the electronic partition function or how to be cautious with mathematics. *European Journal of Physics*, 22(5):483, 2001.

[7] MR Moussa, R Muijlwijk, and H Van Dijk. The vapour pressure of liquid nitrogen. *Physica*, 32(5):900–912, 1966.

[8] Maria Elena Popa, Dipayan Paul, Christof Janssen, and Thomas Röckmann. H2 clumped isotope measurements at natural isotopic abundances. *Rapid Communications in Mass Spectrometry*, 33(3):239–251, 2019.

[9] Michal Przybytek, Wojciech Cencek, Jacek Komasa, Grzegorz Łach, Bogumil Jeziorski, and Krzysztof Szalewicz. Relativistic and quantum electrodynamics effects in the helium pair potential. *Physical review letters*, 104(18):183003, 2010.